

Retinal thinning associates with nigral dopaminergic loss in de novo Parkinson disease

Jeeyun Ahn, MD, PhD,* Jee-Young Lee, MD, PhD,* Tae Wan Kim, MD, PhD, Eun Jin Yoon, PhD, Sohee Oh, PhD, Yu Kyeong Kim, MD, PhD, Jong-Min Kim, MD, PhD, Se Joon Woo, MD, PhD, Ki Woong Kim, MD, PhD, and Beomseok Jeon, MD, PhD

Neurology® 2018;00:e1-e10. doi:10.1212/WNL.00000000000006157

Correspondence

Dr. J.-Y. Lee
wieber04@snu.ac.kr
or Dr. T.W. Kim
twkim93@gmail.com

Abstract

Objective

To analyze the relationship between retinal thinning and nigral dopaminergic loss in de novo Parkinson disease (PD).

Methods

Forty-nine patients with PD and 54 age-matched controls were analyzed. Ophthalmologic examination and macula optical coherence tomography scans were performed with additional microperimetry, *N*-(3-[¹⁸F]fluoropropyl)-2-carbomethoxy-3-(4-iodophenyl) nortropine PET, and 3T MRI scans were done in patients with PD only. Retinal layer thickness and volume were measured in subfields of the 1-, 2.22-, and 3.45-mm Early Treatment of Diabetic Retinopathy Study circle and compared in patients with PD and controls. Correlation of inner retinal layer thinning with microperimetric response was examined in patients with PD, and the relationships between retinal layer thickness and dopamine transporter densities in the ipsilateral caudate, anterior and posterior putamen, and substantia nigra were analyzed.

Results

Retinal layer thinning was observed in the temporal and inferior 2.22-mm sectors (false discovery rate–adjusted $p < 0.05$) of drug-naïve patients with PD, particularly the inner plexiform and ganglion cell layers. The thickness of these layers in the inferior 2.22-mm sector showed a negative correlation with the Hoehn and Yahr stage ($p = 0.032$ and 0.014 , respectively). There was positive correlation between macular sensitivity and retinal layer thickness in all 3.45-mm sectors, the superior 2.22-mm sector, and 1-mm circle ($p < 0.05$ for all). There was an association between retinal thinning and dopaminergic loss in the left substantia nigra (false discovery rate–adjusted $p < 0.001$).

Conclusion

Retinal thinning is present in the early stages of PD, correlates with disease severity, and may be linked to nigral dopaminergic degeneration. Retinal imaging may be useful for detection of pathologic changes occurring in early PD.

RELATED ARTICLE

Editorial

The search for Parkinson disease biomarkers: Retinal thinning as a correlate of dopamine loss

Page 493

*These authors equally contributed to this work.

From the Departments of Ophthalmology (J.A., T.W.K.), Neurology (J.-Y.L.), Nuclear Medicine (E.J.Y., Y.K.K.), and Biomedical Statistics (S.O.), Seoul Metropolitan Government–Seoul National University Boramae Medical Center and Seoul National University College of Medicine; Departments of Neurology (J.M.K.), Ophthalmology (S.J.W.), and Psychiatry (K.W.K.), Seoul National University Bundang Hospital and Seoul National University College of Medicine; and Department of Neurology (B.J.), Seoul National University Hospital and Seoul National University College of Medicine, South Korea.

Go to Neurology.org/N for full disclosures. Funding information and disclosures deemed relevant by the authors, if any, are provided at the end of the article.

Glossary

DAT = dopamine transporter; **ETDRS** = Early Treatment of Diabetic Retinopathy Study; **FDR** = false discovery rate; **18F-FP-CIT** = N-(3-[¹⁸F]fluoropropyl)-2-carbomethoxy-3-(4-iodophenyl) nortropane; **GCL** = ganglion cell layer; **GEE** = generalized estimating equation; **HY** = Hoehn and Yahr; **IPL** = inner plexiform layer; **KLoSHA** = Korean Longitudinal Study on Health and Aging; **LMM** = linear mixed-effects model; **MP** = microperimetry; **NFL** = nerve fiber layer; **OCT** = optical coherence tomography; **ONL** = outer nuclear layer; **PD** = Parkinson disease; **SD** = spectral domain; **WRL** = whole retinal layer.

Visual disturbance is a common nonmotor symptom of Parkinson disease (PD) that is frequently noted from the very early stages of the disease when pathology has not yet expanded to widespread brain areas.¹ Hence, retinal dysfunction and probable pathologic involvement of the retina have been suggested with autopsy studies actually showing decreased retinal dopamine concentrations in patients with PD.^{2,3}

Advances in in vivo imaging technology have enabled the acquisition of high-resolution retinal images using spectral domain (SD)-optical coherence tomography (OCT). Numerous studies have consistently reported morphologic structural changes in the foveal pit and retinal thinning in patients with PD, although there are some conflicts in the results of several earlier studies that may be related to differences in scanning and analysis protocols.^{2,4–13} Earlier studies had only low-resolution time domain-OCT available and did not have automatic segmentation software allowing layer-by-layer analysis.¹⁴ Most studies using SD-OCT reported retinal thinning in PD, which also correlated with disease severity or duration.^{9,12,13,15–19}

Pathologic studies of the retina in PD have been scarce, but recently, α -synuclein pathology was reported in the retina of patients with PD.^{20,21} Retinal degeneration was also demonstrated in the presence of abnormal α -synuclein expression, suggesting a possible mechanism through which pathologic changes take place in the retina of patients with PD.²²

This study aimed to demonstrate inner retinal layer thinning in consecutively recruited drug-naive patients with PD using automated segmentation analysis of each single retinal layer; to apply an advanced statistical model adjusting for age, axial length, and within-participant intereye correlations; to correctly abide by the underlying assumption of independent observations; and then to explore the pathologic implications of retinal thinning by performing a correlation analysis with nigral dopaminergic loss estimated by N-(3-[¹⁸F]fluoropropyl)-2-carbomethoxy-3-(4-iodophenyl) nortropane (¹⁸F-FP-CIT) PET imaging.

Methods

Study participants

Drug-naive patients with de novo PD were consecutively recruited between 2013 and 2014. Patients who visited the movement disorder clinic at Seoul National University

Boramae Medical Center during the study period and were newly diagnosed as having PD were eligible for inclusion. PD diagnosis was made by a movement disorders specialist (J.-Y.L.) on the basis of the clinical diagnostic criteria of the UK PD Brain Bank Society.²³ Controls were voluntarily recruited from either healthy volunteers who visited for routine health checkup or participants of the Korean Longitudinal Study on Health and Aging (KLoSHA) cohort study.²⁴ For every participant with PD, information on age, sex, age at PD onset, and Hoehn and Yahr (HY) stages was collected at the time of diagnosis. Ophthalmologic examinations and image scans were subsequently conducted within 1 month after diagnosis at drug-naive condition.

Exclusion criteria were the presence of comorbid ophthalmic pathologies capable of affecting retinal thickness such as age-related macular degeneration, diabetic retinopathy, retinal vein or artery occlusion, epiretinal membrane, macular hole, high myopia defined as spherical equivalent greater than -6 D or glaucomatous optic neuropathies, presence of media opacity impeding the acquisition of high-quality OCT images, and inability to undergo OCT examination.

Standard protocol approvals, registrations, and patient consents

This study protocol was approved by the Institutional Review Board of our institution, and informed consent was obtained from all participants. The study adhered to the tenets of the Declaration of Helsinki.

Ophthalmologic examinations

All patients underwent comprehensive ophthalmologic examination consisting of best-corrected visual acuity, slit lamp biomicroscopy, indirect fundus exam, axial length measurement (IOLMaster; Carl Zeiss Meditec, Jena, Germany), and SD-OCT (Spectralis OCT; Heidelberg Engineering, Heidelberg, Germany). Patients with PD additionally underwent microperimetry (MP; Spectral OCT/SLO; OPKO-OTI, Miami, FL) in conjunction with the OCT scan.

Optical coherence tomography

High-resolution retinal imaging was performed with the Spectralis OCT. Retinal thickness and volume topographic maps were acquired through raster images consisting of 31 high-resolution B scans covering a $30^\circ \times 25^\circ$ area centered on the fovea. Each scan was 9.00 mm long with an interscan distance of 240 μ m. Retinal thickness was defined as the distance between the surface line of the nerve fiber layer

(NFL) and the hyporeflective line above the retinal pigment epithelium. Using automated segmentation software (Segmentation Technology; Heidelberg Engineering, Inc), we segmented the whole retinal layer (WRL) into the 7 respective retinal layers: the NFL, ganglion cell layer (GCL), inner plexiform layer (IPL), inner nuclear layer, outer plexiform layer, outer nuclear layer (ONL), and photoreceptor layer. We calculated the mean thicknesses and volumes of the WRL and the 7 retinal layers in the 9 sectors of the Early Treatment of Diabetic Retinopathy Study (ETDRS) circle with diameters of 1, 2.22, and 3.45 mm (figure 1).

Microperimetry

MP tests were done with the Polar 3 test pattern, which consists of 28 stimulus points located in 3 concentric rings, 4 central points within 4°, 12 middle points within 8°, and 12 outer points within 12°, centered on the fovea. Because 1° of visual angle is equivalent to $\approx 280 \mu\text{m}$ retinal distance, the 4°, 8°, and 12° concentric rings showed good concordance with the 1-, 2.22-, and 3.45-mm ETDRS circles (figure 1).¹³ Retinal topography map images of the 1-, 2.22-, and 3.45-mm ETDRS circle were overlaid on the MP results on the basis of retinal vessel configuration with care taken that the circle margins matched the 4°, 8°, and 12° concentric rings. A 4-2-1 staircase strategy with stimuli of Goldmann III size, 200-millisecond duration was used, and the stimulus intensity ranged from 0 dB (127 cd/m^2) to 20 dB (2.54 cd/m^2). Intersession repeatability with this MP device has been previously studied, and good agreement in test-retest repeatability has been reported.^{25,26} A representative macular sensitivity value for each ETDRS sector was calculated by averaging the MP thresholds covered by each sector.

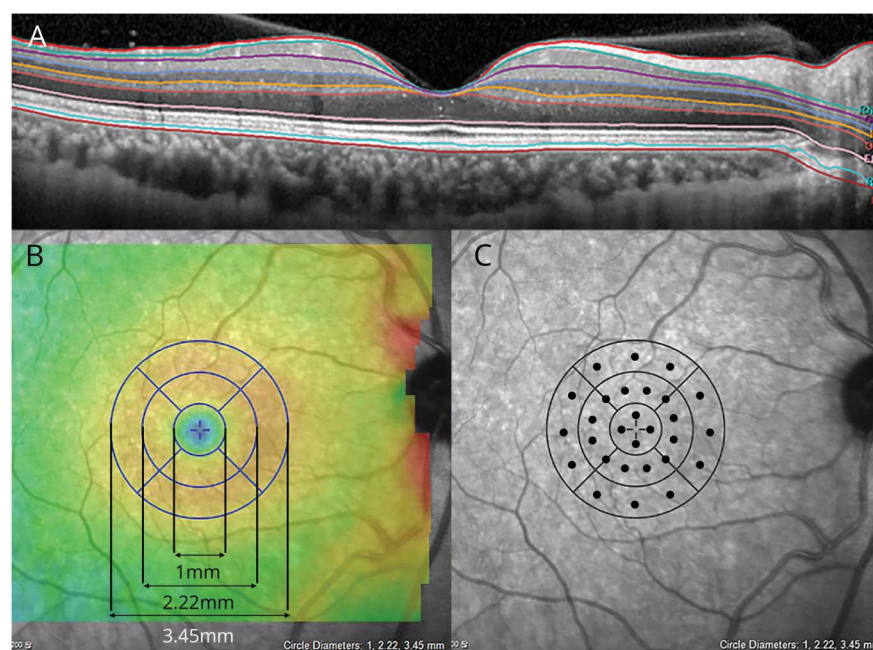
Brain imaging

For the neuroimaging correlation study, 30 patients with PD were randomly selected from the initial eligible cohort during the screening period (figure e-1, links.lww.com/WNL/A659). Each participant underwent PET (Philips Gemini TF-64 PET/CT scanner, Philips Healthcare, Best, the Netherlands) and 3.0T brain MRI (Philips Achieva, Philips Healthcare) in the drug-naive state for either dopaminergic or serotonergic drugs. After bolus injection of 185 MBq ^{18}F -FP-CIT, participants waited for 2 hours and then underwent 10-minute emission scans. After routine corrections for physical effects, images were reconstructed by applying a 3-dimensional row-action maximum-likelihood algorithm for 90 slices, each 2 mm thick, in a 128×128 matrix with corrections for attenuation and scatter. The acquisition parameters for the volumetric T1 MRIs were as follows: repetition time/echo time of 9.9/4.6 milliseconds, flip angle of 8.0°, slice thickness of 1 mm, image matrix of $224 \times 224 \times 180$, and voxel size of $0.98 \times 0.98 \times 1 \text{ mm}^3$.

Estimation of ^{18}F -FP-CIT tracer uptake in brain regions

For the dopamine transporter (DAT) analysis, ^{18}F -FP-CIT tracer uptakes were estimated in the caudate nucleus, anterior and posterior putamen, and substantia nigra of each brain hemisphere with a reference to uptake in the cerebellum as [(average count in region of interest/average count in cerebellum)-1]. Anatomic boundaries for the bilateral caudate, putamen, and cerebellum were made on T1-weighted MRIs by using the FIRST integrated in FSL version 5.0.2. The putamen was divided into anterior and posterior halves along its longitudinal axis. A circular, fixed-size region of interest was

Figure 1 High-resolution retinal imaging performed with Spectralis optical coherence tomography



(A) Built-in automated segmentation software (segmentation technology; Heidelberg Engineering, Inc) was used to delineate all the single retinal layers. (B) Mean thicknesses and volumes of the parafoveal whole retinal layer (WRL), nerve fiber layer (NFL), ganglion cell layer (GCL), inner plexiform layer (IPL), inner nuclear layer (INL), outer plexiform layer (OPL), outer nuclear layer (ONL), and photoreceptor layer (PR) were measured in the 9 sectors of the Early Treatment of Diabetic Retinopathy Study (ETDRS) circle with diameters of 1, 2.22, and 3.45 mm. (C) Retinal topography map images were overlaid on the microperimetry (MP) test results on the basis of retinal vessel configuration, and a representative macular sensitivity value for each ETDRS sector was calculated by averaging the MP thresholds covered by each sector.

set manually for the bilateral substantia nigra on PET-overlaid MRIs with ITK-SNAP software (itk-snap.org). The substantia nigra was identified on 4 transverse slices (1 mm thick for each) with a radius of 4 voxels (169.8 mm³).

Statistical analysis

Selection of statistical analysis approach

For the analysis of ophthalmologic measures, generalized estimating equation (GEE) was chosen to enable adjustment of within-patient intereye correlations and the effect of age and axial length on retinal thickness and volume. As for regression analysis exploring the correlation between retinal thickness and DAT, because retinal layers within a designated sector were analyzed with DAT uptakes of a brain region, the notion that layers are nested within a given sector was contrived, and a linear mixed-effects model (LMM) was used to account for random effects and hierarchy of each retinal layer.

Analysis of ophthalmologic measures

Demographic and ophthalmologic characteristics were compared between patients with PD and controls by the Mann-Whitney *U* test for continuous variables and χ^2 test for categorical variables. Retinal thickness and volume measures of the WRL, as well as each of the 7 segmented layers, were separately compared between patients with PD and controls with the GEE model to account for within-patient intereye correlations and the effect of age and axial length on retinal thickness and volume. In patients with PD, correlation analyses were performed between retinal layer thickness and volume and clinical PD stages assessed with HY stages and between retinal layer thickness and MP values in sector by sector using the Spearman correlation analysis. For the correlation analysis between retinal layer thickness, volume, and clinical PD stages, when both eyes of 1 individual were included, an averaged value of retinal layer thickness and volume was used. For the analysis between retinal layer thickness and MP values, because MP value is an eye-specific variable, there was no averaging of both eye data for a single individual.

Analysis of the retinal thickness in relation to DAT

Simple correlation analysis with retinal thickness measures of the WRL and 7 retinal layers in the 9 EDTRS sectors and DAT uptakes of the caudate nucleus, anterior and posterior putamen, and substantia nigra (both contralateral and ipsilateral to the eyes), involving a total of 1,152 correlations, was carried out. Correlation was found only between the left retina and left hemispheric regions and the right retina and right hemispheric regions ($0.444 \leq r \leq 0.605$, unadjusted $p < 0.05$ by the Spearman method). Therefore, a total of 16 regression analyses were conducted for the ipsilateral measures of the left and right retina thickness values of 9 retinal sectors and the DAT data of 1 region of interest for each of the 4 regions on each side of the brain. Because retinal sectors and layers are nested within each eye and multiple outcomes from the same participant are obtained, LMMs with random effects for participant and for the layers and sectors within each eye were

fitted. Before analyses, retinal thickness and DAT uptake data were transformed to the standardized *z* scores by the use of mean and SD, which were used to assess the relationship between the ipsilateral retinal layer thickness and DAT uptakes in each of the 4 brain regions. The model for retinal thickness considered age and axial length as fixed effects and the DAT values of the region under consideration as random effects. For whole retina thickness, similar LMMs were fitted except without layers. The model diagnostics were examined with residual plots.

Analysis software and *p* value adjustment for multiple comparison

SPSS software (version 19.0, SPSS Inc, Chicago IL) and R version 3.2.1 (r-project.org) were used with the limit of significance set at 0.05 (2 tailed), and multiple comparisons of 7 retinal layers within a sector in thickness and volume comparisons were corrected with the false discovery rate (FDR) method with 0.05 level for the FDR control.²⁷

Data availability

Anonymized data presented in this study will be shared on request to the corresponding authors.

Results

Of the initial 60 eligible patients with PD and 58 controls, 11 patients and 5 controls were excluded from analysis because of inadequate scans, ocular conditions listed in the exclusion criteria, and poor cooperation; 2 of the 11 excluded patients were part of the neuroimaging study. A total of 49 patients with PD (89 eyes) and 54 age-matched controls (108 eyes) were eligible for analysis, and data from 28 (49 eyes) of 30 randomly assigned patients with PD for the neuroimaging study were included in the analysis. Participant enrollment is summarized in figure e-1 (links.lww.com/WNL/A659).

Baseline demographic and ophthalmologic data

Baseline patient demographics and ophthalmologic characteristics are summarized in table 1. There were no differences in age, sex, and spherical equivalent between patients with PD and controls. Patients with PD had slightly longer axial length compared to controls (23.35 ± 0.95 vs 22.95 ± 0.93 , $p = 0.004$). Among patients with PD, there were no differences in baseline factors between those included (28 patients, 49 eyes) and those not included in the neuroimaging study.

Retinal thickness and volume analysis: GEE analysis

WRL thinning was present in the temporal and inferior sectors of the 2.22-mm circle, and the inner retinal layers, NFL, GCL, and IPL also showed thinning (FDR-adjusted $p < 0.05$ for all except the temporal NFL, FDR-adjusted $p = 0.947$) (table 2).

As for retina volume, a similar pattern was observed with decreased volume in the temporal and inferior sectors of the

Table 1 Baseline demographics and ophthalmologic characteristics of participants included in the final analyses

	De novo PD (n = 49, 89 eyes)	Neuroimaging (n = 28, 49 eyes)	Control (n = 54, 108 eyes)	p Value ^a
Age, y	68.9 (9.1)	67.2 (9.7)	70.6 (8.9)	0.385
Male, n (%)	21 (42.9)	13 (46.4)	25 (46.3)	0.726
Age at onset, y	67.4 (9.3)	65.9 (9.8)	NA	NA
Hoehn and Yahr stage	1.8 (0.5)	1.9 (0.5)	NA	NA
Laterality (more affected body side), right: left, n	33:16	17:11	NA	NA
Spherical equivalent, D	0.34 (1.54)	0.28 (1.77)	0.17 (1.08)	0.394 ^b
Axial length, mm	23.35 (0.95)	23.51 (0.90)	22.95 (0.93)	0.004 ^b

Abbreviations: NA = not available; PD = Parkinson disease.

Data shown as mean (SD) unless otherwise indicated; n indicates number of patients.

^a Statistical analysis details are shown in the text. There was no difference in clinical parameters between patients with and those without neuroimaging.

^b Comparison between 89 eyes of patients and 108 eyes of controls.

2.22-mm circle in the NFL, GCL, and IPL layers (FDR-adjusted $p < 0.05$ for all except the temporal NFL, FDR-adjusted $p = 0.173$) (table e-1, links.lww.com/WNL/A660). Full data on thicknesses and volumes for all retinal layers in every sector are presented in table e-1. When the LMM approach was used, there were no significant differences in retina volume (FDR-adjusted $p > 0.05$ for all, data not shown).

Correlation between retinal thickness and PD severity

There was a tendency of negative correlation between thickness of the inner retinal layers in the inferior sector of the 2.22-mm circle and the HY stage ($r = -0.230, -0.361, \text{ and } -0.317$ for NFL, GCL, and IPL; unadjusted $p = 0.123, 0.014, \text{ and } 0.032$, respectively), but no correlation was found between HY and the temporal sector thickness (figure 2).

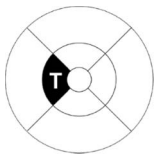
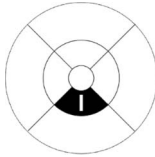
Correlation between retinal thickness and MP

The distribution of MP sensitivity measures in patients with PD for each sector of the 3 circles is shown in figure 3A. Individual variation in MP measures was considerable, especially for those recorded from the 1-mm center circle and from the 2.22-mm circles of the inferior and nasal sectors. There was correlation between MP thresholds and retinal thickness (WRL) in all sectors of the 3.45-mm circle, superior sector of the 2.22-mm circle, and 1-mm center circle (figure 3B).

Retinal thickness and DAT density: Nested LMM analysis

There was an association between retinal thickness and DAT density in the left substantia nigra ($p < 0.001$), whereas in other brain regions, there was no association ($p > 0.05$ for all). Statistics for DAT uptake in the left substantia nigra vs left eye WRL thickness of 9 sectors showed an association only in the

Table 2 Retinal layers with thickness differences between patients with PD and controls

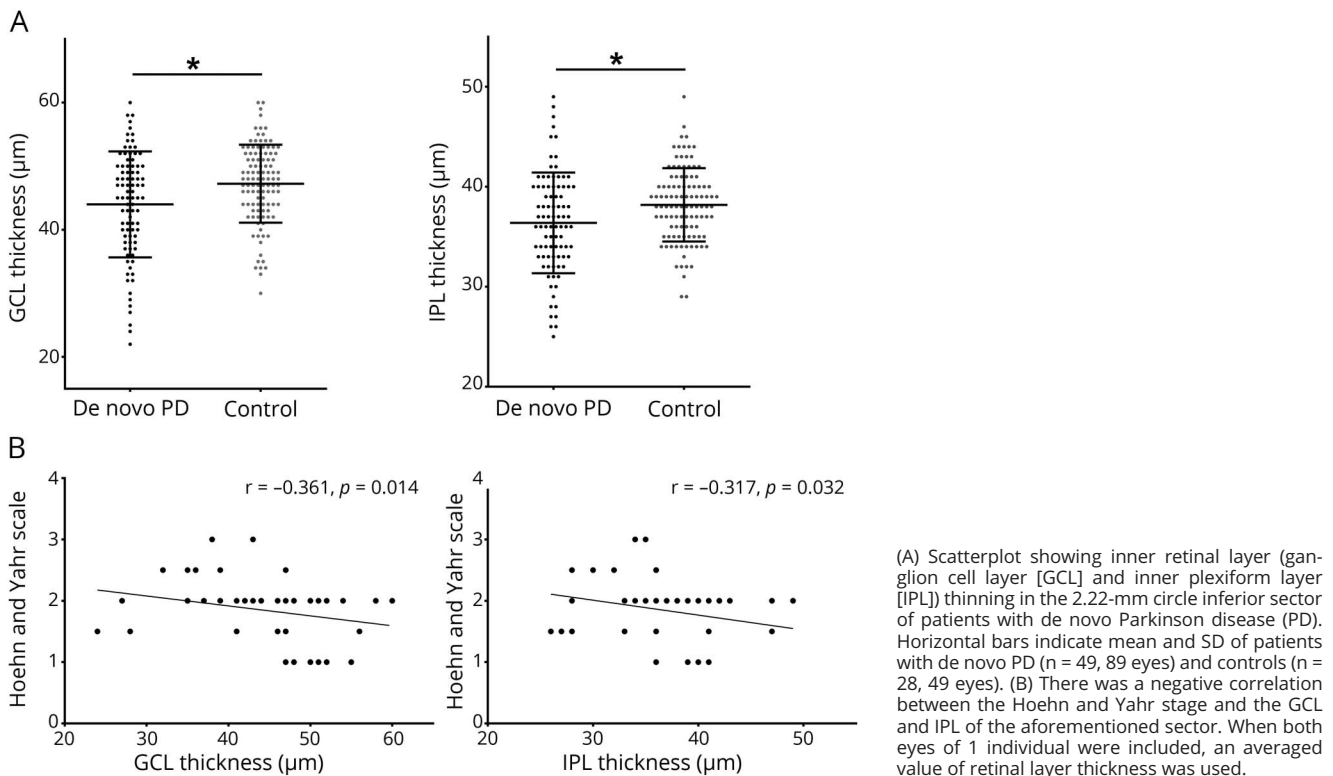
Location	Layer	De novo PD	Control	Unadjusted p value	Adjusted p value ^a
	WRL	313.72 (22.09)	320.10 (17.24)	0.009	NA
	NFL	17.38 (1.87)	17.44 (1.53)	0.894	0.947
	GCL	37.65 (8.46)	40.90 (5.67)	0.002	0.008
	IPL	35.34 (5.05)	37.39 (3.54)	<0.001	0.003
	WRL	323.31 (21.09)	328.72 (17.94)	0.009	NA
	NFL	18.51 (3.02)	19.58 (2.39)	0.005	0.013
	GCL	43.99 (8.34)	47.24 (6.13)	0.001	0.004
	IPL	36.38 (5.03)	38.19 (3.67)	0.001	0.004

Abbreviations: GCL = ganglion cell layer; I = inferior sector; INL = inner nuclear layer; IPL = inner plexiform layer; NA = not available; NFL = nerve fiber layer; PD = Parkinson disease; T = temporal sector; WRL = whole retinal layer.

Data are shown as mean (SD) unless otherwise indicated.

^a Analysis was done with generalized estimating equations adjusted for age and axial length. False discovery rate-adjusted p values for multiple comparison of 7 retinal layers within a sector are shown.

Figure 2 Retinal thinning and correlation with PD severity



inferior sector of the 2.22-mm circle ($p = 0.0372$). The LMM for 7 individual retinal layers of 9 sectors vs DAT uptakes in the left substantia nigra also showed associations in the inferior sector of the 2.22-mm circle (table 3), not in other sectors. There was a positive association in the inner retinal layers (NFL, GCL, IPL, and inner nuclear layer), whereas in the ONL, there was a negative association (FDR-adjusted p for all < 0.05 , table 3). The diagnostics of the fitted LMM model constructed for the left substantia nigra vs left eye retinal individual layer thicknesses are summarized in the supplementary material (links.lww.com/WNL/A661).

Discussion

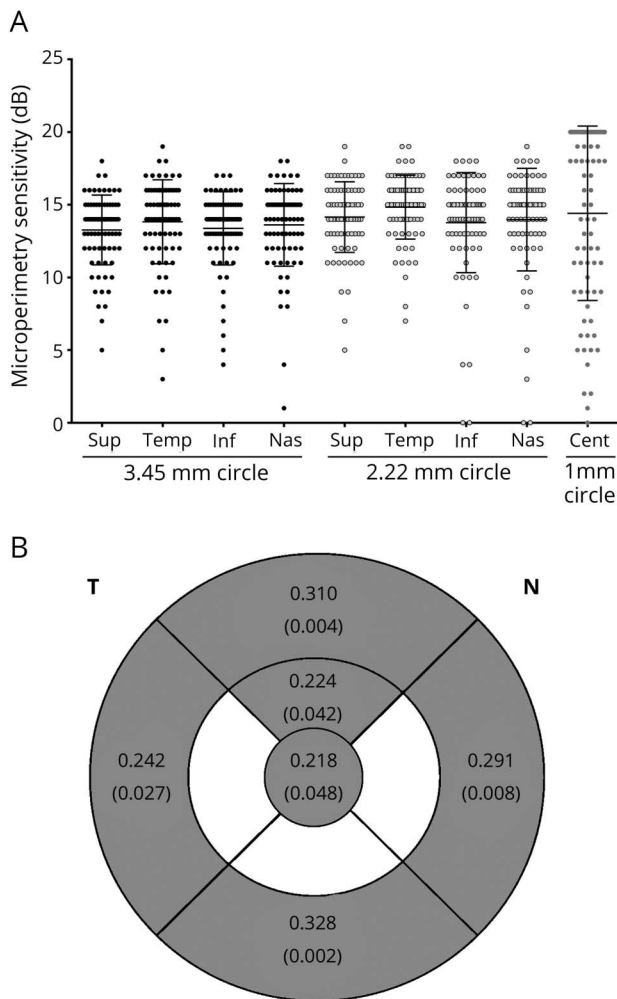
This study showed retinal thinning in drug-naive patients with PD that was apparent in the inner retinal layers of the inferior and temporal sectors of the 2.22-mm circle. Inner retinal layer thinning, especially the GCL and IPL in the inferior sector, showed correlation with the HY stage and DAT loss in the substantia nigra, raising the possibility of a pathologic interconnection between the retina and nigral dopaminergic cell degeneration in PD. In addition, we found correlations between retinal thickness and MP thresholds, possibly demonstrating the functional implications of structural retinal change.

The strength of the present study is that we used a high-resolution OCT device with built-in automated segmentation

software, making analysis of each retinal layer more accurate and reliable.²⁸ To avoid possible bias from antiparkinsonian medications and ophthalmologic conditions, we included only drug-naive patients at the early stage of the disease and those without ophthalmologic diseases as mentioned, and we implemented an advanced statistical model to control for the effects of age and axial length, both known to have a significant impact on retinal thickness.

Inner retinal thinning in patients with PD has been reported in other studies conducting segmental layer analysis or separate analysis of the inner and outer layers.^{12,13,19} The inner retinal layers are of interest because this is the region in which not only dopaminergic cells are present but also α -synuclein pathologies have been reported.^{20,21,29} The present study showed the relationship between inner retinal thinning and nigral dopaminergic neuronal loss within the brain for the first time. The correlation of retinal thinning with DAT loss was ascertained in the substantia nigra but not in the striatal regions by the nested LMM analysis. Striatal DAT density reflects striatal dopamine depletion but does not correlate well with the viable nigral cell count in either PD primate models³⁰ or humans.³¹ In addition, studies have shown compensatory DAT downregulation in the distal axons of dopaminergic neurons to the striatum in drug-naive patients with PD.³² Hence, nigral DAT imaging is believed to be a reliable biomarker for viable neuronal count.^{33–35} In that sense, our study results may be evidence for a possible

Figure 3 Microperimetry (MP) response: individual distribution and correlation with retinal thickness. (A) Scatterplot of microperimetry (MP) response according to different sectors of the Early Treatment of Diabetic Retinopathy Study (ETDRS) circle



(A) Scatterplot of MP response according to different sectors of the Early Treatment of Diabetic Retinopathy Study (ETDRS) circle. Horizontal bars indicate mean and SD. Cent = center; Inf = inferior sector; Nas = nasal sector; Sup = superior sector; Temp = temporal sector. (B) Results of the correlation analyses between the whole retinal thickness and MP sensitivity are depicted in the ETDRS circle. There was significant correlation between MP thresholds and whole retinal thickness in all sectors of the 3.45-mm circle, superior sector of the 2.22-mm circle, and 1-mm center circle (significant sectors shaded in gray). Spearman correlation coefficient is given in each respective sector with the *p* value in parentheses. Because MP value is an eye-specific variable, there was no averaging of both eye data for a single individual. N = nasal; T = temporal.

pathologic interconnection between the retina and brain in PD. However, there are several findings that need further investigation.

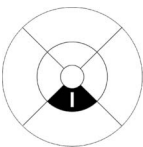
Although ONL thickness was not significantly reduced in patients with PD, it showed a negative relation with DAT uptake. The reduction in inner retinal layer thickness may be compensated for by relative thickening of the outer layer, as has also been postulated in earlier studies.^{36–38} In addition, a retina-DAT correlation was found on the left side but not on

the right side of the retina-brain. Such laterality predilection is possibly due to the nearly 2-fold recruitment of patients with symptom onset in the right side of the body in the present study (table 1) and can be explained by the postulation that the retina, as with the substantia nigra, may be affected asymmetrically in the early stages of PD (supplementary reference, links.lww.com/WNL/A662). In support of this hypothesis, there has been a report on interocular foveal thickness asymmetry in PD.³⁹ Further studies with larger numbers and balanced patients with affected body side involvement will, we hope, provide more insight into this issue.

Inner retinal changes tended to occur in the macular region in patients with PD. Frequent visual symptoms in PD such as visual acuity decline, impaired contrast sensitivity and color discrimination, and visual perceptual dysfunctions could be linked to this pattern of retinal thinning. Retinal thinning was detected in the inferior and temporal 2.22-mm sectors in our patients, showing that retinal involvement in early PD is likely to be focal rather than diffuse. It is possible that this topographic pattern of retinal thinning is random rather than preferential because other OCT studies including patients with more advanced stages of PD report changes in other sectors as well.^{6,40,41} Whether the detection of subtle changes in the retina for early-stage PD is more feasible in the inferior and temporal sectors with OCT scans because retinal degeneration follows a certain sequential pattern in PD remains a topic that needs to be addressed in future studies using novel retinal ganglion cell imaging techniques more precisely at the cellular level.⁴²

Direct structural-functional correlation was feasible through sector-by-sector analyses of the MP thresholds and OCT results. There are only a few functional correlation studies in relation to retinal thickness in PD so far. Functional tests used in those studies^{12,13,17,43} were visual acuity, contrast sensitivity, and color discrimination, which were limited in controlling for the effect of brain function. One study reported a weak correlation between multifocal electroretinogram, an objective measure of foveal cone function, and OCT changes of the inner retinal layers.¹⁷ However, previous functional studies were unable to show the topography of structural-functional correlations, which is important because retinal structural change occurs unevenly throughout different regions of the macula. MP is a psychophysical subjective response to a threshold stimulus, and therefore, MP sensitivity is affected by not only the retina but also brain function. However, because all sectors are equally influenced by brain function in a single individual, this confounding effect can be controlled for by performing correlation analysis at the sector level. Function studies on visual symptoms can also be affected by dopaminergic medications. Thus, we included only patients with de novo PD who had never been treated with antiparkinsonian drugs. There was also wide variation in individual responses in MP. This is not reported in normal individuals but can be related to retinal comorbidity because certain lesions occurring in age-related macular degeneration

Table 3 Sectors with an association between individual retinal layer thickness of the left eye and DAT uptakes in the left substantia nigra in patients with de novo PD

Sectors	Layers	Estimate	Standard error	Degrees of freedom	t Value	95% Confidence interval		Unadjusted <i>p</i> value	Adjusted <i>p</i> value ^a
						Lower	Upper		
	NFL	0.463	0.210	1,384	2.208	-0.052	0.875	0.0274	0.0469
	GCL	0.447	0.210	1,384	2.128	0.035	0.858	0.0335	0.0469
	IPL	0.456	0.210	1,384	2.174	0.045	0.868	0.0298	0.0469
	INL	0.479	0.210	1,384	2.282	0.067	0.890	0.0227	0.0469
	OPL	0.391	0.210	1,384	1.863	-0.021	0.802	0.0627	0.0732
	ONL	-0.456	0.210	1,384	-2.176	-0.868	-0.045	0.0297	0.0469
	PR	-0.293	0.210	1,384	-1.396	-0.705	0.119	0.1628	0.1628

Abbreviations: DAT = dopamine transporter; GCL = ganglion cell layer; I = inferior sector; INL = inner nuclear layer; IPL = inner plexiform layer; NFL = retinal nerve fiber layer; ONL = outer nuclear layer; OPL = outer plexiform layer; PD = Parkinson disease; PR = pigmented epithelium layer.

^a Analysis was done with multivariate nested linear mixed-effects models. The model for retinal thickness considered age and axial length as fixed effects and DAT values of each region of interest, layer within sector, and individual variability as random effects. False discovery rate-adjusted *p* values for multiple comparison of 7 retinal layers within a sector are shown.

have been associated with greater variability in MP sensitivity.^{25,44} This may also be driven by individual patient variability in having steady fixation, but the variation was widest in the central circle, followed by measures in the 2.22-mm circle nasal and inferior sectors (figure 3A). It could be inferred that foveal remodeling into a wider pit, as reported in patients with PD by several studies,² may result in increased variability of the foveal slope. Therefore, when we exert single-point stimulations, the response may vary, depending on the slope change at that point. We averaged MP values from 3 to 4 points within a sector rather than estimating the MP sensitivity of the whole area of the sector because of technical restraints, thereby making it more difficult to find significant correlations with the current method.

One MPTP animal model study showed that retinal thinning detected on an OCT device can actually reflect pathologic degeneration of the retina.⁴⁵ Recently, retinal thinning on OCT images was revealed to correspond to retinal ganglion cell loss in patients with multiple system atrophy,⁴⁶ although there is no human study providing such evidence in PD. There are several reports on α -synuclein pathology in the retina of patients with PD.^{20,21,47} One study reported α -synuclein-positive inclusions in the inner retinal layers of 3 patients with PD,²⁰ while another study found no abnormal staining of α -synuclein in 6 patients with PD.⁴⁷ However, a recent study using retinal whole-mount and immunohistochemical method targeting phosphorylated α -synuclein showed retinal phosphorylated α -synuclein-positive fibers in retinal ganglion cells specifically in 7 of 9 patients with PD, in 1 of 3 patients with dementia with Lewy bodies, and in no controls or patients with Alzheimer disease.²¹ Because phosphorylation at serine 129 is detected only in humans with α -synucleinopathies,⁴⁸

these observations are probably pathologic findings rather than the effect of aging alone. With recent in vivo imaging techniques, α -synuclein aggregates were also visualized in the retinal ganglion cells in α -synuclein transgenic mouse with increased accumulation with age.⁴⁹ In a rotenone-induced rodent model of PD, retinal ganglion cell complexes degenerated earlier than neuronal cells in the substantia nigra, suggesting that retinal change may precede brain pathology in PD.⁵⁰ However, more human studies are warranted to confirm this assumption, and if retinal change is pathologically linked to α -synuclein pathology and nigral dopaminergic loss in PD, in vivo retinal imaging could be a useful biomarker for monitoring disease progression or measuring the efficacy of neuroprotective therapeutics in PD. It could also be used for early diagnosis in the premotor stages of PD, although there is still much room for improvement with regard to OCT resolution to make this feasible.

Our study results need to be interpreted with caution. Retinal analysis was confined to the macular area because it is not yet technically feasible to scan the whole convex retina. However, functional impairments in relation to central vision have been raised in patients with PD so far, and central vision is the most vital part of an individual's visual function. Thus, our study design could be justified for focusing on the macular scan. The present study focused on thickness and volume changes, but future studies incorporating the 3-dimensional structural changes involving the foveal pit would provide additional insight. DAT imaging was performed in only randomly selected 50% of eligible patients with PD. This sample size was predetermined for the minimum number of participants required for PET analysis considering both the cost-effectiveness of our research and the pilot nature of this study. Thus, further studies with a larger number of patients would help to verify our

findings. In addition, this was a cross-sectional study, so retinal structural changes in correlation with PD severity need to be confirmed through longitudinal follow-up studies.

In vivo application of SD-OCT is a safe and noninvasive technique with enhanced reproducibility and reliability using automated segmentation software. On the basis of the present study results, automatic measures of the inner retinal layer thickness, particularly in the inferior sectors near the foveal area, may be suggested as a candidate biomarker for early PD that may also reflect nigral dopaminergic cell loss. Further studies are needed to validate this finding and to show longitudinal change of OCT measures along the progression of the disease.

Author contributions

J.A., J.Y.L., and T.W.K. designed the study and contributed to data analysis and interpretation, with substantial contributions from all the coauthors. J.A., J.Y.L., T.W.K., E.J.Y., Y.K.K., S.J.W., and K.W.K. collected the data. J.M.K. and B.J. supervised the study. J.A. and S.O. did the statistical analysis. J.A. and J.Y.L. drafted the manuscript to which all coauthors contributed revisions. All authors approved the final version.

Study funding

This work was supported by a clinical research grant-in-aid from the Seoul Metropolitan Government Seoul National University Boramae Medical Center (03-2015-8) and a National Research Foundation grant funded by the Ministry of Education, Science and Technology in Korea (NRF-2018R1C1B3008971).

Disclosure

J. Ahn, J. Lee, T.W. Kim, E. Yoon, S. Oh, Y.K. Kim, and J.M. Kim report no disclosures relevant to the manuscript. S. Woo received honoraria from Samsung Bioepis and Retimark Inc. K.W. Kim and B. Jeon report no disclosures relevant to the manuscript. Go to Neurology.org/N for full disclosures.

Received November 21, 2017. Accepted in final form June 7, 2018.

References

1. Archibald NK, Clarke MP, Mosimann UP, Burn DJ. Visual symptoms in Parkinson's disease and Parkinson's disease dementia. *Mov Disord* 2011;26:2387–2395.
2. Harnois C, Di Paolo T. Decreased dopamine in the retinas of patients with Parkinson's disease. *Invest Ophthalmol Vis Sci* 1990;31:2473–2475.
3. Bodis-Wollner I. Retinopathy in Parkinson disease. *J Neural Transm* 2009;116:1493–1501.
4. Hajee ME, March WF, Lazzaro DR, et al. Inner retinal layer thinning in Parkinson disease. *Arch Ophthalmol* 2009;127:737–741.
5. Archibald NK, Clarke MP, Mosimann UP, Burn DJ. Retinal thickness in Parkinson's disease. *Parkinsonism Relat Disord* 2011;17:431–436.
6. Albrecht P, Muller AK, Sudmeyer M, et al. Optical coherence tomography in parkinsonian syndromes. *PLoS One* 2012;7:e34891.
7. Bodis-Wollner I. Foveal vision is impaired in Parkinson's disease. *Parkinsonism Relat Disord* 2013;19:1–14.
8. Adam CR, Shrier E, Ding Y, Glazman S, Bodis-Wollner I. Correlation of inner retinal thickness evaluated by spectral-domain optical coherence tomography and contrast sensitivity in Parkinson disease. *J Neuroophthalmol* 2013;33:137–142.
9. Lee JY, Kim JM, Ahn J, Kim HJ, Jeon BS, Kim TW. Retinal nerve fiber layer thickness and visual hallucinations in Parkinson's disease. *Mov Disord* 2014;29:61–67.

10. Lee JY, Ahn J, Kim TW, Jeon BS. Optical coherence tomography in Parkinson's disease: is the retina a biomarker? *J Parkinsons Dis* 2014;4:197–204.
11. Nowacka B, Lubinski W, Honczarenko K, Potemkowski A, Safranow K. Bioelectrical function and structural assessment of the retina in patients with early stages of Parkinson's disease (PD). *Doc Ophthalmol* 2015;131:95–104.
12. Pilat A, Proudlock FA, Gottlob I. Reply. *Ophthalmology* 2016;123:e20.
13. Ucak T, Alagoz A, Cakir B, Celik E, Bozkurt E, Alagoz G. Analysis of the retinal nerve fiber and ganglion cell: inner plexiform layer by optical coherence tomography in Parkinson's patients. *Parkinsonism Relat Disord* 2016;31:59–64.
14. Bodis-Wollner I, Miri S, Glazman S. Venturing into the no-man's land of the retina in Parkinson's disease. *Mov Disord* 2014;29:15–22.
15. Jimenez B, Ascaso FJ, Cristobal JA, Lopez del Val J. Development of a prediction formula of Parkinson disease severity by optical coherence tomography. *Mov Disord* 2014;29:68–74.
16. Satue M, Seral M, Otin S, et al. Retinal thinning and correlation with functional disability in patients with Parkinson's disease. *Br J Ophthalmol* 2014;98:350–355.
17. Kaur M, Saxena R, Singh D, et al. Changes in Parkinson disease. *J Neuroophthalmol* 2015;35:254–258.
18. Mailankody P, Battu R, Khanna A, Lenka A, Yadav R, Pal PK. Optical coherence tomography as a tool to evaluate retinal changes in Parkinson's disease. *Parkinsonism Relat Disord* 2015;21:1164–1169.
19. Garcia-Martin E, Larrosa JM, Polo V, et al. Distribution of retinal layer atrophy in patients with Parkinson disease and association with disease severity and duration. *Am J Ophthalmol* 2014;157:470–478 e2.
20. Bodis-Wollner I, Kozlowski PB, Glazman S, Miri S. α -Synuclein in the inner retina in Parkinson disease. *Ann Neurol* 2014;75:964–966.
21. Beach TG, Carew J, Serrano G, et al. Phosphorylated alpha-synuclein-immunoreactive retinal neuronal elements in Parkinson's disease subjects. *Neurosci Lett* 2014;571:34–38.
22. Feany MB, Bender WW. A Drosophila model of Parkinson's disease. *Nature* 2000;404:394–398.
23. Hughes AJ, Daniel SE, Kilford L, Lees AJ. Accuracy of clinical diagnosis of idiopathic Parkinson's disease: a clinico-pathological study of 100 cases. *J Neurol Neurosurg Psychiatry* 1992;55:181–184.
24. Jhoo JH, Kim KW, Huh Y, et al. Prevalence of dementia and its subtypes in an elderly urban Korean population: results from the Korean Longitudinal Study on Health and Aging (KLoSHA). *Dement Geriatr Cogn Disord* 2008;26:270–276.
25. Zadlo A, Szweczyk G, Sarna M, et al. Photoaging of retinal pigment epithelial melanosomes: the effect of photobleaching on morphology and reactivity of the pigment granules. *Free Radic Biol Med* 2016;97:320–329.
26. Olchawa MM, Pilat AK, Szweczyk GM, Sarna TJ. Inhibition of phagocytic activity of ARPE-19 cells by free radical mediated oxidative stress. *Free Radic Res* 2016;50:887–897.
27. Benjamini Y, Hochberg Y. Controlling the false discovery rate: a practical and powerful approach to multiple testing. *J R Statist Soc B* 1995;57:289–300.
28. Bittersohl D, Stemplewitz B, Keseru M, Buhmann C, Richard G, Hassenstein A. Detection of retinal changes in idiopathic Parkinson's disease using high-resolution optical coherence tomography and Heidelberg retina tomography. *Acta Ophthalmol* 2015;93:e578–e584.
29. Witkovsky P. Dopamine and retinal function. *Doc Ophthalmol* 2004;108:17–40.
30. Karimi M, Tian L, Brown CA, et al. Validation of nigrostriatal positron emission tomography measures: critical limits. *Ann Neurol* 2013;73:390–396.
31. Saari L, Kivinen K, Gardberg M, Joutsa J, Noponen T, Kaasinen V. Dopamine transporter imaging does not predict the number of nigral neurons in Parkinson disease. *Neurology* 2017;88:1461–1467.
32. Lee CS, Samii A, Sossi V, et al. In vivo positron emission tomographic evidence for compensatory changes in presynaptic dopaminergic nerve terminals in Parkinson's disease. *Ann Neurol* 2000;47:493–503.
33. Perlmutter JS, Norris SA. Neuroimaging biomarkers for Parkinson disease: facts and fantasy. *Ann Neurol* 2014;76:769–783.
34. Strafella AP, Bohnen NI, Perlmutter JS, et al. Molecular imaging to track Parkinson's disease and atypical parkinsonisms: new imaging frontiers. *Mov Disord* 2017;32:181–192.
35. Benamer HT, Patterson J, Wyper DJ, Hadley DM, Macphie GJ, Grosset DG. Correlation of Parkinson's disease severity and duration with ¹²³I-FP-CIT SPECT striatal uptake. *Mov Disord* 2000;15:692–698.
36. Gabriel R, Lesauter J, Banvolgyi T, Petrovics G, Silver R, Witkovsky P. All amacrine neurons of the rat retina show diurnal and circadian rhythms of parvalbumin immunoreactivity. *Cell Tissue Res* 2004;315:181–186.
37. Schneider M, Muller HP, Lauda F, et al. Retinal single-layer analysis in parkinsonian syndromes: an optical coherence tomography study. *J Neural Transm* 2014;121:41–47.
38. Muller AK, Blasberg C, Sudmeyer M, Aktas O, Albrecht P. Photoreceptor layer thinning in parkinsonian syndromes. *Mov Disord* 2014;29:1222–1223.
39. Shrier EM, Adam CR, Spund B, Glazman S, Bodis-Wollner I. Interocular asymmetry of foveal thickness in Parkinson disease. *J Ophthalmol* 2012;2012:728457.
40. Feany MB. Studying human neurodegenerative diseases in flies and worms. *J Neuropathol Exp Neurol* 2000;59:847–856.
41. Garcia-Martin E, Rodriguez-Mena D, Satue M, et al. Electrophysiology and optical coherence tomography to evaluate Parkinson disease severity. *Invest Ophthalmol Vis Sci* 2014;55:696–705.

42. Nalls MA, Pankratz N, Lill CM, et al. Large-scale meta-analysis of genome-wide association data identifies six new risk loci for Parkinson's disease. *Nat Genet* 2014;46:989–993.
43. Roth NM, Saidu S, Zimmermann H, et al. Photoreceptor layer thinning in idiopathic Parkinson's disease. *Mov Disord* 2014;29:1163–1170.
44. Sulzbacher F, Kiss C, Kaider A, et al. Correlation of SD-OCT features and retinal sensitivity in neovascular age-related macular degeneration. *Invest Ophthalmol Vis Sci* 2012;53:6448–6455.
45. Schneider JS, Ault ME, Anderson DW. Retinal Pathology detected by optical coherence tomography in an animal model of Parkinson's disease. *Mov Disord* 2014;29:1547–1551.
46. Mendoza-Santesteban CE, Palma JA, Ortuno-Lizaran I, Cuenca N, Kaufmann H. Pathologic confirmation of retinal ganglion cell loss in multiple system atrophy. *Neurology* 2017;88:2233–2235.
47. Ho CY, Troncoso JC, Knox D, Stark W, Eberhart CG. Beta-amyloid, phospho-tau and alpha-synuclein deposits similar to those in the brain are not identified in the eyes of Alzheimer's and Parkinson's disease patients. *Brain Pathol* 2014;24:25–32.
48. Beach TG, Adler CH, Sue LI, et al. Multi-organ distribution of phosphorylated alpha-synuclein histopathology in subjects with Lewy body disorders. *Acta Neuropathol* 2010;119:689–702.
49. Price DL, Rockenstein E, Mante M, et al. Longitudinal live imaging of retinal alpha-synuclein: GFP deposits in a transgenic mouse model of Parkinson's disease/dementia with Lewy bodies. *Sci Rep* 2016;6:29523.
50. Normando EM, Davis BM, De Groef L, et al. The retina as an early biomarker of neurodegeneration in a rotenone-induced model of Parkinson's disease: evidence for a neuroprotective effect of rosiglitazone in the eye and brain. *Acta Neuropathol Commun* 2016;4:86.